Multi-Photon Effects in Inclusive and Semi-Inclusive Deep Inelastic Scattering
PAC 53

D. Gaskell*, T.J. Hague†, S. Covrig Dusa, R. Ent, D. W. Higinbotham, D. Mack, S. Malace, C. Morean, and A. Panta

Thomas Jefferson National Accelerator Facility, Newport News, VA 23606, USA

M. Nycz*

University of Virginia, Charlottesville, VA 22903, USA

N. Fomin and D. Nguyen

University of Tennessee, Knoxville, TN 37996, USA

J. Arrington, P. Datta, and S. Li

Lawrence Berkeley National Laboratory, Berkeley, CA 94720, USA

E. Kinney

University of Colorado, Boulder, CO 80309, USA

T. Horn

The Catholic University of America, Washington, DC 20064, USA

P. Markowitz

Florida International University, Miami, FL 33199, USA

A. Hoghmrtsyan, A. Mkrtchyan, H. Mkrtchyan, and V. Tadevosyan

A. I. Alikhanyan National Science Laboratory (Yerevan Physics Institute), Yerevan 0036, Armenia

M. Elaasar

Southern University at New Orleans, New Orleans, LA 70126, USA

D. Adhikari

Virginia Tech, Blacksburg, VA 24061, USA

S. Bhattarai

Idaho State University, Pocatello, ID, 83209, USA

D. Androić

University of Zagreb, Zagreb, Croatia

A. Afanasev

The George Washington University, Washington, DC 20052, USA

B. Duran

New Mexico State University, Las Cruces, NM 88003, USA

S. Alsalmi

Department of Physics and Astronomy, College of Science, King Saud University, Riyadh 11451, Saudi Arabia

H. Bhatt

Mississippi State University, Mississippi State, MS 39762, USA

*: Spokesperson, †: Contact-spokesperson (tjhague@jlab.org)

A Positron Working Group Proposal

Executive Summary

The magnitude of hard two-photon exchange effects is a subject of debate in elastic scattering due to the well-known discrepancy between Rosenbluth-separation and polarization transfer measurements of the form factor ratio. Even less known in the contribution of these effects to inelastic scattering. In nuclear targets, these multi-photon effects get combined with effects due to the charge of the nucleus to describe what are colloquially referred to as "Coulomb Corrections". This proposal aims to measure two-photon exchange effects in deep inelastic scattering and semi-inclusive deep inelastic scattering as well as Coulomb Correction effects in semi-inclusive deep inelastic scattering.

Currently, there is an almost complete lack of data in order to constrain these effects. While hard two-photon exchange is ignored in typical radiative correction prescriptions, Coulomb Corrections are applied through the improved effective momentum approximation (the Improved EMA). The Improved EMA has been shown to work well for quasi-elastic scattering, but is untested in inelastic scattering. The EMA formalism will be tested in inclusive scattering from nuclear targets in experiment C12+23-003 [1], but there is no reason to expect that the approximation will work well for semi-inclusive deep inelastic scattering where the final state is substantially more complicated than inclusive measurements.

These measurements will allow us to characterize and constrain these effects, giving improved confidence in past, current, and future inelastic scattering measurements. Deep inelastic and semi-inclusive deep inelastic scattering, being key to the study of nuclear and nucleon structure, are high priority to understand and to support the mission of JLab. The most clear and direct impact of these measurements will be on the results of the upcoming $R = \sigma_L/\sigma_T$ measurements (E12-06-104 [2], E12-24-001 [3], and E12-14-002 [4]) in Hall C. These experiments will use a Rosenbluth-separation technique (LT separation) to extract R_H, R_D, and $R_A - R_D$ in deep inelastic and semi-inclusive deep inelastic scattering.

LT separation measurements are particularly sensitive to ε-dependent effects, that is effects that depend on the helicity of the virtual photon exchanged. Two-photon exchange effects are expected to be directly dependent on ε, which means that their exclusion could dramatically change the results of LT separation measurements if the effects are sizable. While Coulomb Correction effects do not *directly* depend on ε, relative magnitude scales inversely with the beam energy and the scattered lepton energy, the parameters that are adjusted to access different ε values at constant x and Q^2.

These effects, being charge-odd, are able to be directly accessed with the availability of a positron beam at JLab. For electromagnetic interactions, the ratio of positron to electron cross sections will only deviate from unity due to the magnitude of these charge-odd effects. These measurements are of critical importance to correctly analyze and interpret past and future nuclear physics data both at JLab and beyond.

To complete these measurements we request a total of 58.4 days of beam time in Hall C using the standard HMS and SHMS equipment and three targets: a 10cm hydrogen target, a 10cm empty cell, and a 6% RL copper target. 50.8 days of a 1 μA positron beam will be required, divided between 5 beam energies (4.4, 5.5, 6.5, 8.6, and 10.7 GeV). 7.5 days of a 25 μA electron beam will be required, divided between 5 beam energies (4.4, 5.5, 6.5, 8.6, and 10.7 GeV). This time will be used, for each beam type, to record 9 data points of π^+ SIDIS on hydrogen, 3 data points of $\pi-$ SIDIS on hydrogen, 5 data points of π^+ SIDIS on copper, and 34 data points of inclusive DIS on hydrogen (5 which are taken simultaneously with the SIDIS data).

Contents

1 Physics Motivation

1.1 Elastic Two-Photon Exchange

For over 70 years, understanding the internal structure of the nucleon has been at the forefront of nuclear physics research, with the electric and magnetic form factors of the proton, G_E and G_M, playing a fundamental role in this pursuit. Through elastic scattering of leptons from a proton target, G_E and G_M have been commonly extracted over these 70 years using a technique known at LT or Rosenbluth separation. An LT separation requires making measurements of the reduced cross section at constant four-momentum transfer (Q^2) as a function of ε. The reduced cross section can be expressed as

$$\frac{d\sigma}{d\Omega_e} = \frac{\sigma_{Mott}}{\varepsilon\,(1+\tau)}\left[\tau G_M^2(Q^2) + \varepsilon G_E^2(Q^2)\right], \tag{1}$$

where σ_{Mott} is the Mott cross section, $\tau = \frac{Q^2}{4M_p^2}$, and ε is given by

$$\varepsilon = [1 + 2(1+\tau)\tan^2(\theta/2)]^{-1}. \tag{2}$$

The linear nature of the reduced cross section, which can be seen in Equation 1 and observed Figure 1, allows for the extraction of both G_E^2 and G_M^2 through a linear fit.

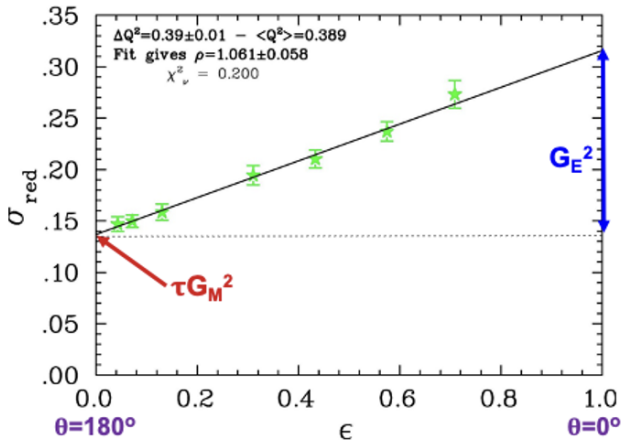

Figure 1: Illustration of a typical Rosenbluth separation used to measure nucleon form factors. By measuring the reduced cross section at fixed Q^2 across a range of ε values, the form factors can be extracted for a linear fit.

Alternatively, the direct ratio, G_E/G_M, can be measured using various polarization techniques. One such method is polarization transfer, in which a longitudinally polarized electron scatters off of a unpolarized proton target, and the polarization of the scattered proton is measured. The ratio G_E/G_M is given by:

$$\frac{G_E}{G_M} = -\frac{P_t}{P_l}\frac{E+E'}{2M}\tan\theta/2. \tag{3}$$

These two methods should produce identical G_E/G_M ratios, but it was found that there was a discrepancy at values of Q^2 above 1 GeV^2 [5, 6]. This discrepancy is shown in Figure 2.

Since this discrepancy was first discovered over 25 years ago, a concerted effort has been made to understand the underlying source. The source of the discrepancy has been attributed to hard two-photon exchange effects (TPE), which are believed to be small but are also inherently model dependent. Due to the model dependence of these corrections, they are not included in the standard radiative corrections used in experimental analyses. To understand the effect of a small TPE correction to the ratio G_E/G_M, one can look at the different LT separations made at unique Q^2 values, as shown in Figure 3. One can see that at increasingly higher Q^2 (0.7,1.190,and 2.287 (GeV/c)^2 respectively), the contribution of G_E^2 to the total cross section is significantly diminished as compared to that of G_M^2.

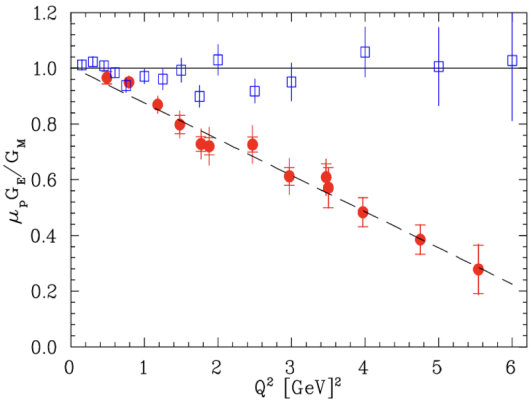

Figure 2: Discrepancy in the proton form factor ratio, G_E/G_M, between Rosenbluth and Polarization transfer measurements

Depending on the exact size of the TPE effect, combined with any ε dependence of the TPE effect, it is apparent how a small effect can have a large impact to the extracted G_E^2. G_E^2 may contribute 5% to the reduced cross section at high Q^2, while the effect of TPE can similarly be on the order of several percent.

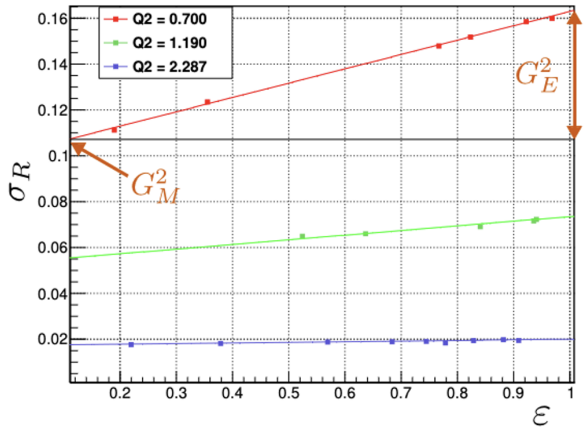

Figure 3: The contribution of G_E to the reduced cross section for different Q^2 values. G_E is greatly diminished with increasing Q^2, illustrating how a small (percent level) TPE correction could result in the observed Rosenbluth/PT discrepancy.

As shown in Figure 1, Rosenbluth measurements are sensitive to G_E^2 and G_M^2, while polarization transfer (PT) measurements probe directly the ratio G_E/G_M. The direct ratio from PT measurements is believed to be less sensitive to TPE effects.

1.1.1 Measurements and Theoretical Predictions of TPE in Elastic Scattering

Measurements of the $\frac{e^+}{e^-}$ cross section ratio provide direct access to the real part of the TPE and the magnitude of the effect. This is illustrated in Equation 4.

$$R_{2\gamma} = \frac{\sigma_{e^+}}{\sigma_{e^-}} \approx 1 + \frac{4Re[M_{\gamma\gamma}M_{\gamma}]}{|M_{\gamma}|}. \tag{4}$$

Recent experiments (references for Vepp-3, clas, olympus) have made $\frac{e^+}{e^-}$ measurements to determine the size of the TPE effect. Figures 4,5 illustrate both the ε and Q^2 coverage of the three experiments, showing the measurements were made at relatively low Q^2 and high ε, outside of the region where TPE are expected to be large.

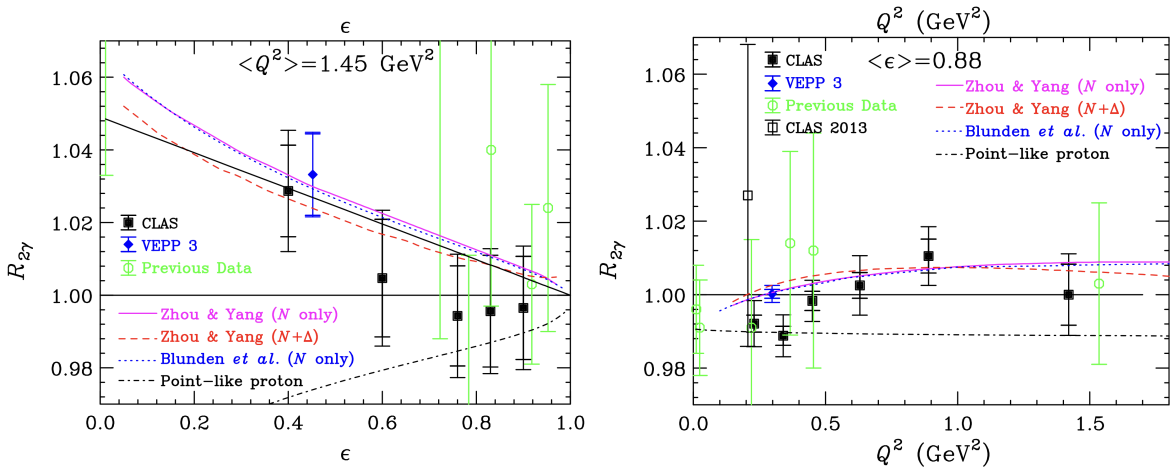

Figure 4: VEPP 3 [7] and CLAS [8] $\frac{e^+}{e^-}$ measurements, shown together along with theoretical predictions for the expected size of the two-photon exchange. The range in Q^2 is below where the discrepancy between LT and polarization transfer is large and at higher values ε, where TPE is expected to be smaller.

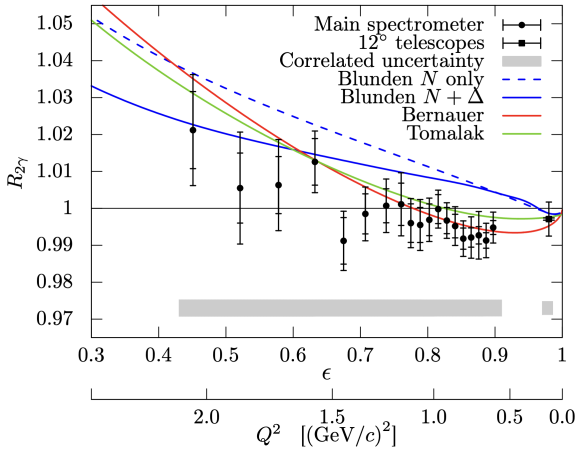

Figure 5: Results from the Olympus experiment [9]. The range in Q^2 is below where the discrepancy between LT and polarization transfer is large and at higher values ε, where TPE is expected to be smaller.

On the theoretical side, a number of approaches have been made. These include one-loop methods to evaluate the box and cross boxed TPE terms (as shown in Fig. 6), dispersion relations, and QCD based approaches at moderate to large Q^2. A comparison of a selected number theoretical and phenomenological models at two Q^2 values are shown in Figure 7. As can be seen, while overall agreement exists among the calculations for a non-zero TPE correction, the size and ε dependence can differ significantly.

1.2 Inelastic Two-Photon Exchange

While there is exists no conclusive evidence implicating the effects of the two-photon exchange effect as the source of the discrepancy in the ratio G_E/G_M, the overwhelming consensus of both experimentalists and theorists is that it is due to unaccounted for hard two-photon exchange terms. This leads to a question about the possible impact that two-photon exchange may have on other reactions, namely deep-inelastic (DIS) and semi-inclusive deep-inelastic (SIDIS) scattering. No corollary exists in either DIS or SIDIS to that of polarization transfer in elastic scattering that would allow for such a comparison. A limited number of experiments have been performed to measure the TPE in DIS and

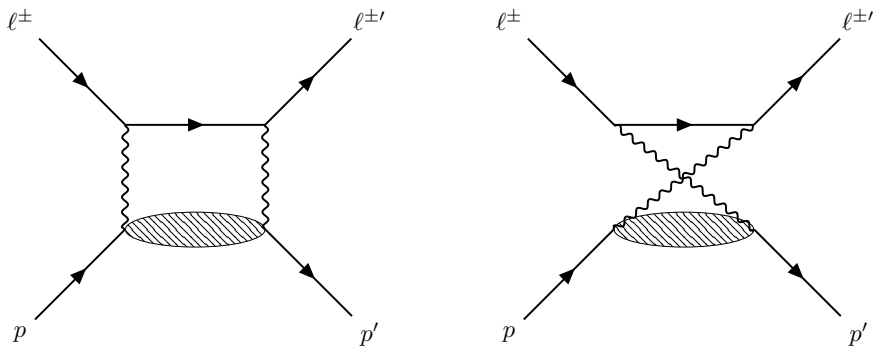

Figure 6: Two Photon Exchange box and cross boxed diagrams [10].

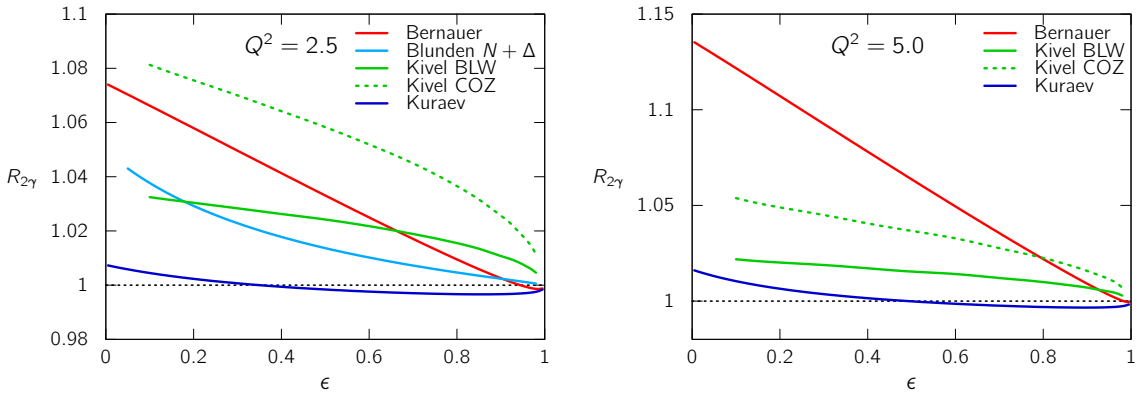

Figure 7: The estimated two-photon exchange contribution to the positron-to-electron cross section ratio for a range of calculations and extractions at $Q^2 = 2.5$ and 5 GeV^2 [11, 12, 13, 14]

can be divided into those that probe either the real or imaginary part of the TPE. Figure 8 shows the results of an experiment which performed μ^+ and μ^- scattering to make a direction measurement of the magnitude of the TPE is DIS through $\frac{\mu^+}{\mu^-}$ ratios [15]. The experiment measured the structure functions νW_2^+ and νW_2^-, where $W_2^+(W_2^-)$ is the structure function from $\mu^+(\mu^-)$ scattering. They then formed an asymmetry of these structure functions,

$$\epsilon = \frac{\nu W_2^+ - \nu W_2^-}{\nu W_2^+ + \nu W_2^-}. \tag{5}$$

Note that in the above equation, we have used ϵ for the asymmetry to maintain consistent notation with the source, but this is *not* the same as the photon helicity fraction denoted by ε in all other locations in this proposal.

The bottom panel of Figure 8 illustrates their final results. They estimate that the contribution from two-photon exchange effects are less than 1.7%. Additional measurements are critically needed to validate this measurement. Also, as observed in elastic LT measurement, a small effect, even at the level of 1.7%, can still have a large effect in LT separations.

Figure 9 are results from target-normal single spin asymmetry (TNSSA) measurements, which is sensitive to the imaginary part of TPE [16, 17]. These measurements require a target which is polarized normal to the scattering plane along with an unpolarized lepton beam. In the Born Approximation, the asymmetry between opposite transverse target settings can be written as

$$A_y = \frac{\sigma^{\uparrow} - \sigma^{\downarrow}}{\sigma^{\uparrow} + \sigma^{\downarrow}}, \tag{6}$$

where $\sigma^{\uparrow}$ and $\sigma^{\downarrow}$ correspond to the cross section of an unpolarized electron scattering off of a nucleon spin polarized parallel or anti-parallel to the scattering plan. In the Born approximation, this asymmetry is zero due to time-reversal and parity conservation (add citation, crist-lee, etc..). A non-zero

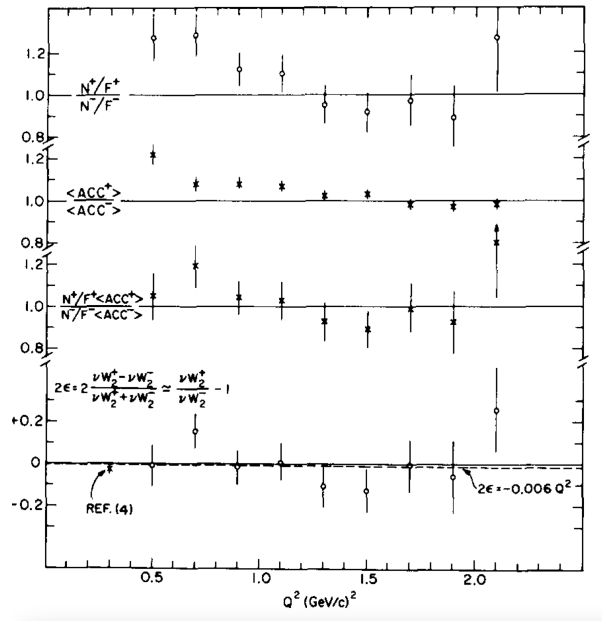

Figure 8: The ratio of μ^+ and μ^- scattering. The bottom line shows the asymmetry between μ^+ and μ^-, from which TPE effects were estimated to be less than 1.7% [15].

asymmetry would be due to two-photon exchange. The plots on the left of Figure 9 are TNSSA results from HERMES [16] on the proton, which were found to be consistent with zero while those on the right are those from JLab and measured a non-zero asymmetry of the neutron at a 2.89σ level, providing the first indication of two-photon exchange in DIS [17].

Finally, there have been no measurements of TPE in SIDIS. There are few estimates on the potential impact of TPE on SIDIS LT separation. Recent predictions for TPE in SIDIS, shown in Fig. 10, calculate a very large effect that will be clearly visible in our experiment, if correct.

1.3 Coulomb Corrections in Inelastic Scattering

"Coulomb Corrections" refers to the effect of acceleration of charged probes in the Coulomb field of a nuclear target. The presence of additional protons in the nucleus (beyond the struck nucleon) leads the exchange of soft photons that distort the initial and final wavefunctions of the probe. In essence, electrons gain energy before scattering and lose energy after scattering while positrons experience the opposite effect due to the sign change of the charge [20].

The applicability and formulation of Coulomb Corrections to inelastic scattering is not well understood and tested even less. In 1978, leading order Coulomb Corrections to deep inelastic electron and muon scattering were calculated and it was found that "the net result is too small to be experimentally significant" [21]. However, evaluating the expressions therein using "typical" JLab kinematics yields corrections that are substantial when compared to "typical" JLab precision.

For a coherent historical perspective of the current best practices related to Coulomb Corrections, we must discuss quasi-elastic scattering. An experiment using Carbon-12 and Lead-208 at the Saclay Linear Accelerator (ALS), tested Coulomb Correction calculations in quasi-elastic scattering by measuring cross sections with both an electron and a positron beam [22]. These results, seen in Fig. 11, were then used to discriminate between different models and found that the Effective Momentum Approximation (EMA) best described the data. The EMA seeks a more readily calculated prescription of the Coulomb Corrections calculated from the Distorted Wave Born Approximation (DWBA) [23, 24, 25]. In this formalism, the measured incoming and outgoing probe momenta are modified at the vertex to an "effective momentum" calculated from nuclear properties and the cross section is then scaled by a "focusing factor". In noting some deficiencies in the EMA, it was then further modified to the Improved EMA (IEMA). The IEMA scales down the Coulomb potential, V_0, to $\overline{V}$ by noting that the scattering does not occur at the center of the potential [26]. The corrected cross section in the IEMA

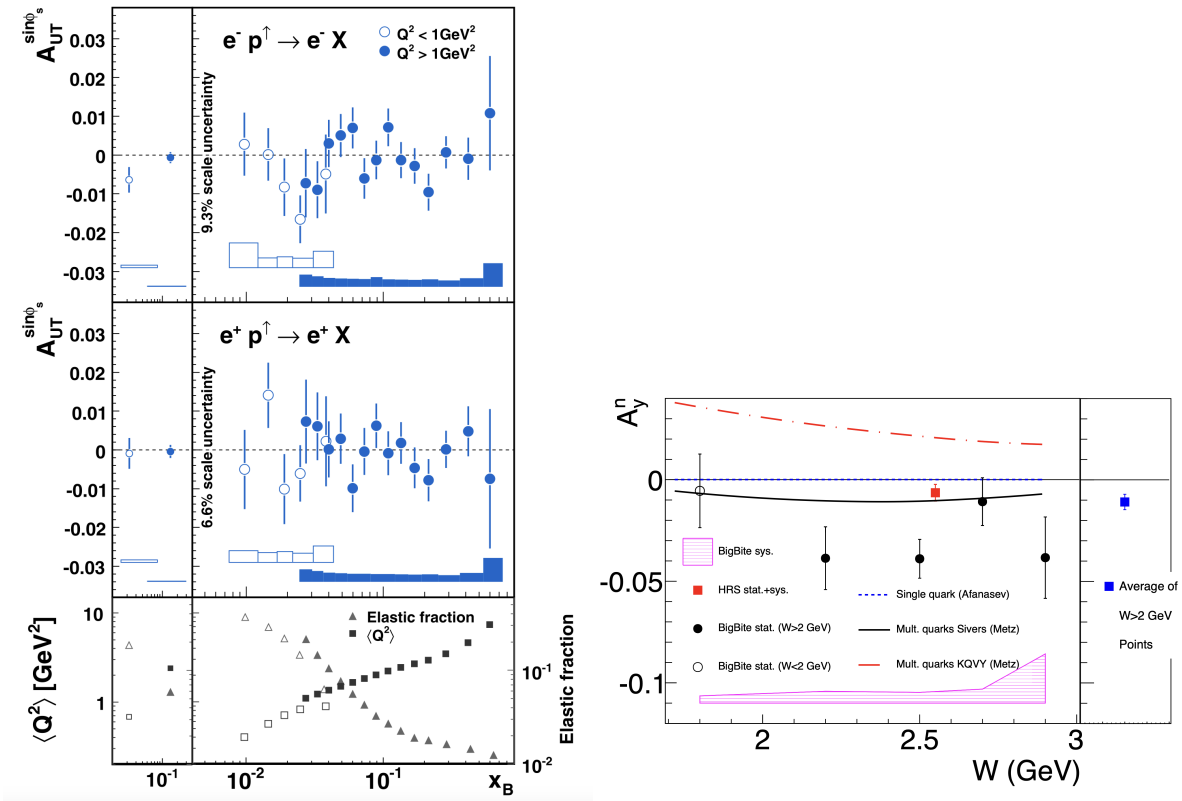

Figure 9: Measurements of the target-normal single spin asymmetry in deep inelastic scattering. The plot on the measurements of the TNSSA of the proton [16] while those on the right are the TNSSA of the neutron and are non-zero at 2.89σ level[17]

is described by

$$\sigma_C = F^2 \sigma \left(E_0 + \overline{V}, E' + \overline{V} \right), \tag{7}$$

where

$$\overline{V} = (0.7 - 0.8)\, V_0, \tag{8}$$

$$V_0 = \frac{3\alpha Z}{2R}, \tag{9}$$

and the focusing factor is given by

$$F^2 = \left(1 + \frac{V_0}{E_0} \right)^2. \tag{10}$$

In the above equations, E_0 is the beam energy, E' is the scattered probe energy, Z is the atomic number of the nuclear target, and R is the radius of the nucleus.

It should be stressed that while the IEMA is an effective tool for applying Coulomb Corrections to quasi-elastic scattering, it is not a realistic representation of the process that occurs. The calculations have been tuned so that they approximately reproduce the results of DWBA calculations. While the description provides a seemingly intuitive mental picture of the process, it is not a correct picture leading to the natural conclusion that we have very little reason to believe that the same procedure should apply in DIS and SIDIS where the underlying process is fundamentally different.

Despite this, there exist no detailed calculations of Coulomb Corrections in the inelastic regime (DIS nor SIDIS). The typical procedure for inelastic scattering at JLab is to use the IEMA. It has been shown to bring data sets into internal agreement, such as in Ref. [20] where E03-103 preliminary data on Gold recorded at 40° and 50° are shown before and after correction (shown here in Fig. 12). However, this application still leaves tension with past SLAC data, suggesting that this may not be a complete description. PAC51 approved an experiment to study Coulomb Corrections in the DIS regime [1]. These corrections are even less studied in the SIDIS reaction and it is logical to question

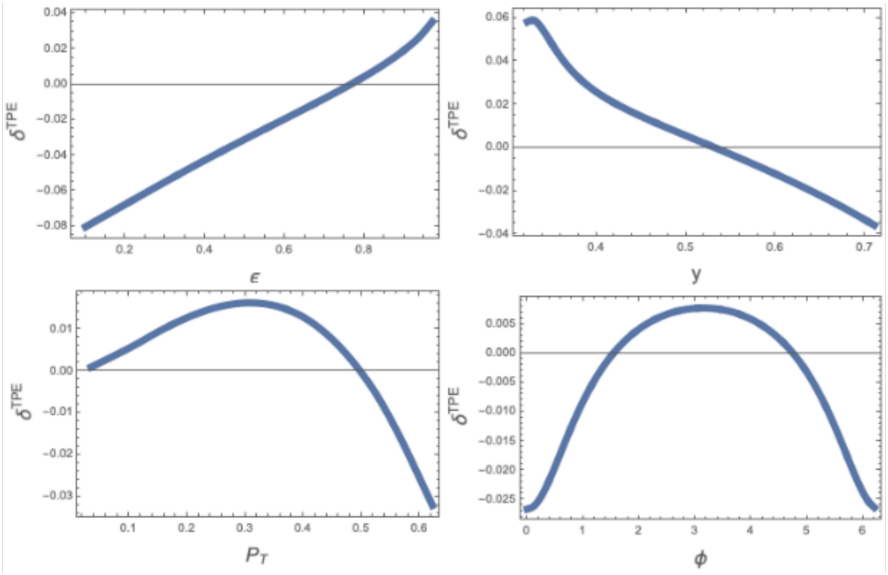

Figure 10: Predictions for the two photon exchange effect in SIDIS at $x = 0.31$, $Q^2 = 2.5$ GeV^2, and $z = 0.5$. Figure from Refs. [18, 19].

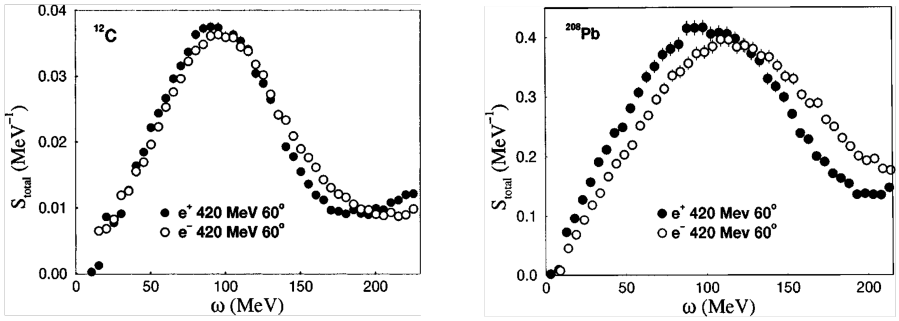

Figure 11: Comparison of electron and positron scattering in Carbon-12 and Lead-208 from Ref. [22]. These data validated that the EMA works well in quasi-elastic scattering.

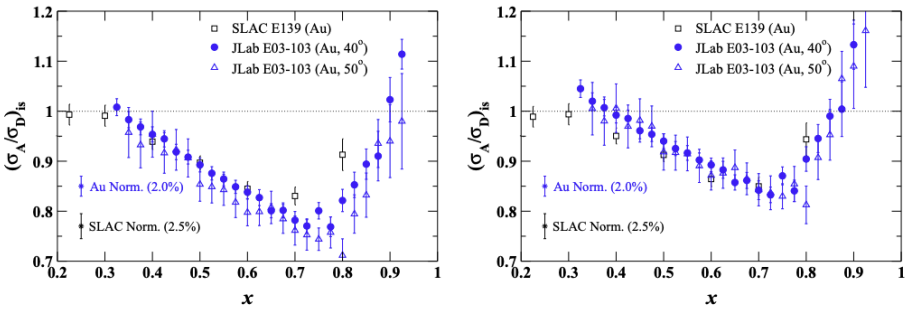

Figure 12: Preliminary E03-103 data on Gold at different kinematics from Ref. [20]. Coulomb Corrections bring the data into internal agreement. However, there is still tension with SLAC data.

whether the corrections would be different in SIDIS due to the substantial restriction on the phase space of the hadronic final state. This proposal aims to complementarily study Coulomb Corrections in SIDIS in order to ensure that we are correctly treating past and future JLab data.

As formulated, the IEMA is an inherently ε-dependent effect. While V_0 and $\overline{V}$ are constant for any given target, by applying them additively they are fractionally larger corrections when E_0 or E' are smaller.

1.4 Impact of this measurement

1.4.1 LT Separations

Two-Photon Exchange and Coulomb Corrections, as epsilon dependent effects, will have direct impacts on LT separation measurements. LT separation refers to the measurement of $R = \sigma_L/\sigma_T$, the ratio of cross sections for longitudinal and transverse helicity virtual photons. The differential cross section for the absorption of longitudinal and transverse virtual photons can be written as:

$$\frac{d^2\sigma}{d\Omega dE'} = \Gamma[\sigma_T(x,Q^2) + \varepsilon\sigma_L(x,Q^2)]. \tag{11}$$

It is a standard assumption that this value is the same for all nuclei and for all inelastic processes. However, this assumption is poorly constrained and experiments E12-06-104 [2], E12-14-002 [4], and E12-24-001 [3] aim to explore whether this assumption is valid. If these experiments find that R shows any nuclear or process dependence, it will have far reaching implications for the extraction of nuclear structure and our understanding of the EMC effect.

LT extractions use a Rosenbluth-like technique to extract σ_L and σ_T, or $R_A - R_D$ in the case of the nuclear measurements. This technique exploits that the contribution of σ_L scales linearly with ε. As such, any ε-dependent effects can meaningfully affect the interpretation of the results. Figure 13 illustrates the LT separation in inclusive DIS for 3 different settings (constant x and Q^2) from experiment E140 at SLAC [27]. This experiment made measurements of the reduced cross section of deuterium, iron and gold, over a x and Q^2 range of 0.2-0.5 and 1.0-5.0 GeV^2, respectively, to determine any possible kinematic or nuclear dependence of $R = \sigma_L/\sigma_T$ in deep inelastic scattering.

While there have been several measurements of $R = \sigma_L/\sigma_T$ and $R_A - R_D$ in DIS [27, 28, 29], in semi-inclusive deep inelastic scatter, much less is known. Figure 14 shows the data collected at the Wilson Synchrotron Laboratory at Cornell University in the late 1970s in blue and red[30, 31, 32], along with projections for experiment E12-06-104 in black. The level of precision of the current data is quite limited and will be greatly improved upon by the E12-06-104 experiment.

Underlying future precision LT separation experiments in both DIS and SIDIS is our knowledge of (or lack of) TPE effects and their impact on the extractions of σ_L and σ_T. Measurements of σ_L/σ_T in both DIS and SIDIS, will be obscured without an understanding of TPE and CC effects. This can plainly be seen in Fig. 15, reproduced from Ref. [35], that shows the impact of Coulomb Corrections on an R_{LT} extraction. These plots show that without Coulomb Corrections (left) the data is, to 0.16σ, consistent with no nuclear dependence to R_{LT}, as is typically assumed. However, on the right it is shown that the application of Coulomb Corrections via the IEMA leads to a 1.2σ deviation from

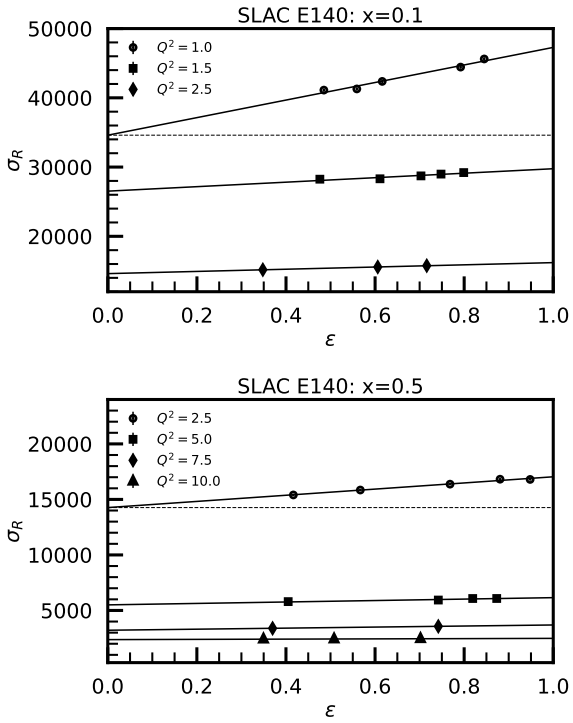

Figure 13: SLAC E140 R_{LT} extractions from [27]

the no nuclear dependence assumption. As TPE correction predictions are even larger than IEMA CC corrections, it is of critical importance that we measure these to ensure we arrive at a correct interpretation of R_{LT} data.

1.4.2 Hadron Attenuation

An accurate measurement of R_{LT} in SIDIS is critical to the study of hadron attenuation. Hadron attenuation is the study of how the nuclear medium affects the formation of hadrons in inelastic scattering. This is studied through the double ratio,

$$R_A^h = \frac{\frac{N_h}{N_e}\Big|_A}{\frac{N_h}{N_e}\Big|_D} = \frac{\frac{d\sigma}{dz}\Big|_A}{\frac{d\sigma}{dz}\Big|_D}, \tag{12}$$

where N_h is the yield of h hadrons and N_e is the inclusive DIS electron yield. The numerator is the yield ratio for a nucleus A and the denominator is for a deuterium nucleus. Studying hadron attenuation for differently sized nuclei allows for investigating the length scale of hadronization. Shorter length scales suggest that hadron attenuation is dominated by hadronic interactions whereas longer length scales would be dominated by partonic interactions.

The naive quark-parton model then allows this double ratio to be related to parton-distribution functions (PDFs) and fragmentation functions (FFs) by

$$\frac{d\sigma}{dz} \sim \sum_q e_q^2 q(x, Q^2) D_{q\to h}(z, Q^2). \tag{13}$$

However, this standard relation hinges on the assumption that $R_{LT}^{SIDIS} = R_{LT}^{DIS}$. Should this equality not hold *or* if there is a nuclear dependence to R_{LT}, fragmentation functions will be extracted incorrectly from SIDIS data. SIDIS data on hadron attenuation has also been used to constrain the properties of hadron production such as from HERMES [36] and CLAS [37] shown in Figs. 16 and 17, respectively.

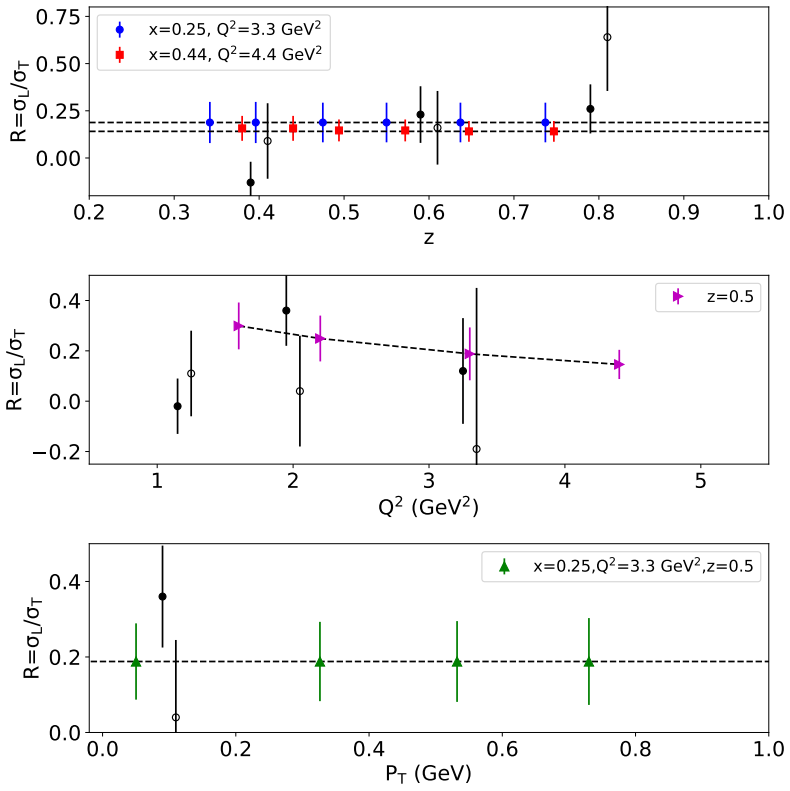

Figure 14: Existing data on $R = \sigma_L/\sigma_T$ from Cornell [33, 34] (black circles) with projections for Hall C E12-06-104 (blue, red, magenta and green points).

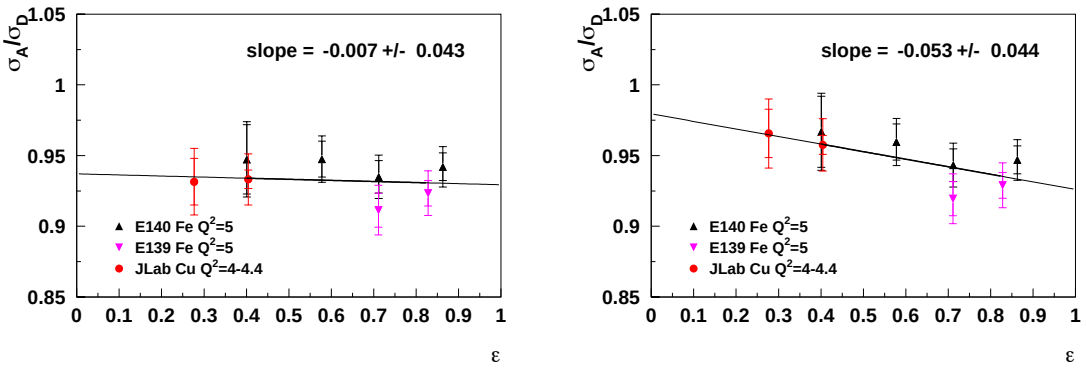

Figure 15: *Left:* σ_A/σ_D for iron and copper DIS data plotted versus ε with no Coulomb Corrections applied. The slope is proportional to $R_A - R_D$. A non-zero slope implies a nuclear dependence for R_{LT}. Without Coulomb Corrections, the slope is consistent with 0. *Right:* The same data with Coulomb Corrections applied using the IEMA. This shows that if the IEMA is valid in inelastic scattering it can clearly change the interpretation of the data to suggest a nuclear dependence for R_{LT}. Figure from Ref. [35].

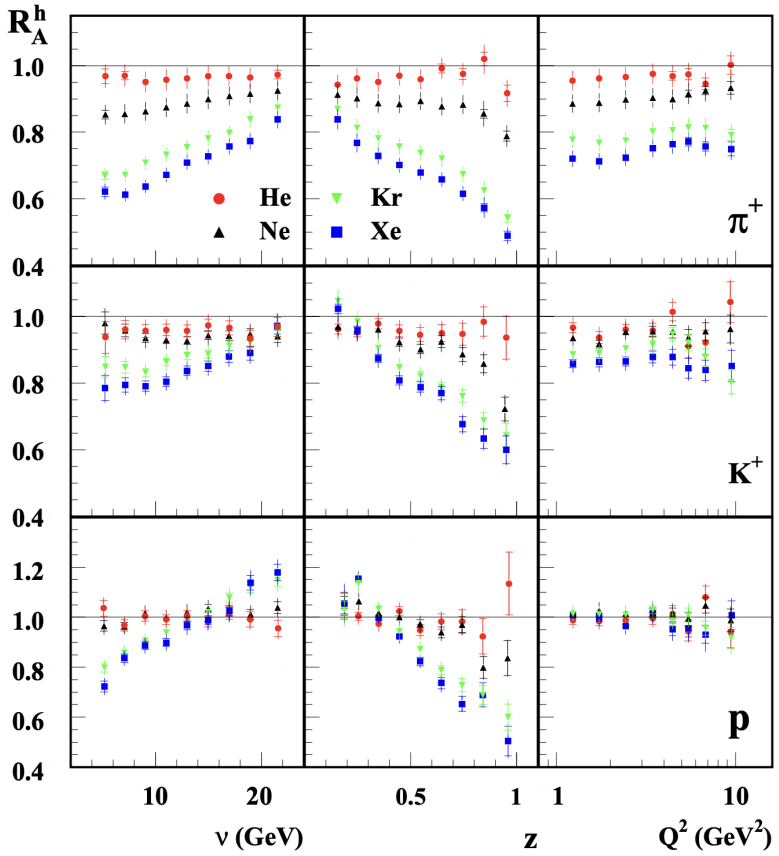

Figure 16: Hadron attenuation ratio results from HERMES for a variety of nuclei with each row as a different hadronic final state. These results are plotted with respect to energy transfer ν, hadronic energy fraction z, and four-momentum transfer squared Q^2. Figure from Ref. [36].

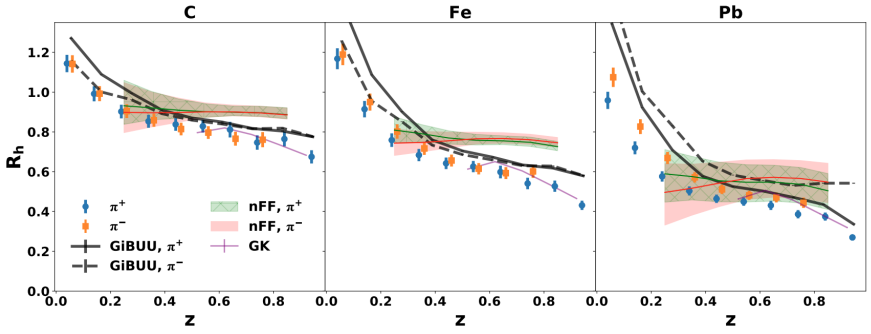

Figure 17: Hadron attenuation ratio results from CLAS for a variety of nuclei for charged pion SIDIS data. Figure from Ref. [37]

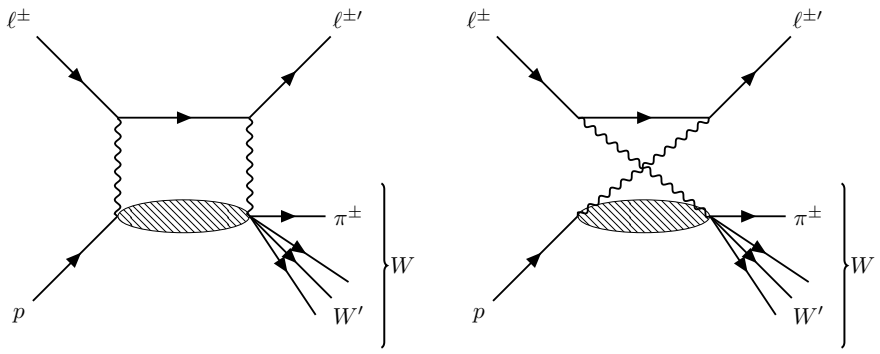

Figure 18: SIDIS Two Photon Exchange box and cross boxed diagrams [10].

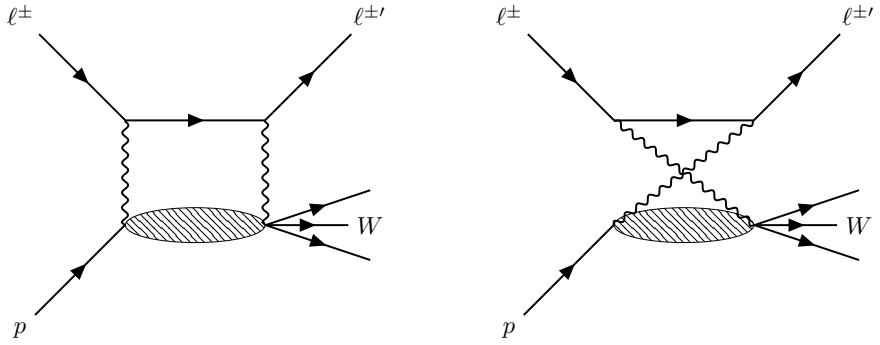

Figure 19: DIS Two Photon Exchange box and cross boxed diagrams [10].

2 Experimental Details

To study two photon exchange and Coulomb effects, this experiment will measure the ratios of positron to electron cross sections for both DIS and SIDIS. These effects are charge-odd and will therefore not cancel in this ratio.

For two-photon exchange effects, we will use a hydrogen target for both DIS and SIDIS (diagrams shown in Figs. 18 and 19). In both cases, we define the ratio

$$R_{2\gamma} = \frac{\sigma_{e^+}}{\sigma_{e^-}} \approx 1 - 2\delta_{2\gamma} \tag{14}$$

where $\delta_{2\gamma}$ is the TPE correction.

For Coulomb Corrections, we will use ratios of nuclear targets to hydrogen. These will then be used to form an e^+/e^- double ratio of the form

$$R_{CC} = \frac{\left(\frac{\sigma_A}{\sigma_H}\right)^{e^+}}{\left(\frac{\sigma_A}{\sigma_H}\right)^{e^-}}. \tag{15}$$

In this double ratio, details of the nuclear structure will cancel. What remains is the difference in Coulomb corrections for a given nuclear target. As Coulomb effects are a function of the charge in a nucleus, it is dependent on atomic number Z. The effect will be enhanced by choosing a high Z target, leading to our decision to use copper. Copper provides the best figure of merit for this study by having a high target thickness per radiation length, allowing us to have a high physics rate while not increasing the target radiation length so much as to introduce very large systematic uncertainties from radiative corrections.

2.1 Required Equipment

This proposal is planned around using the JLab Hall C standard equipment, that is the High Momentum Spectrometer (HMS) and Super High Momentum Spectrometer (SHMS). This setup will use the HMS for detecting scattered beam leptons and the SHMS for detecting final state pions. The data requires 5 positron beam energies and 5 electron beam energies to acquire the necessary data 4.4, 5.5, 6.5, 8.6, and 10.7 GeV [38]. All estimates for rate and beam time assume a 1 μA positron beam and a 25 μA electron beam. Note that while the experiment would benefit from a dedicated device for measuring the beam current at small values (i.e. 1 μA), this proposal does not assume that such a device is available.

2.1.1 Targets

This proposal makes use of three targets: a 10cm hydrogen target, a 10cm empty target cell, and a 6% RL copper foil. The hydrogen target is necessary for the TPE studies as well as a baseline for the CC studies. The empty target is necessary for assessing the cell wall background in the hydrogen data. The copper foil will be used for a subset of the kinematics to study CC in SIDIS.

2.2 Electron Data

This proposal has been planned in such a way that the measurement will be impactful if an electron beam is not available within the same run period. This is done by mimicking the kinematics and target choices of JLab Hall C experiments E12-06-104, E12-24-001, and E12-14-002. However, it is highly preferable to do this experiment when data can be recorded with both positrons and electrons in the same run period and we are requesting the time necessary for that. The target thickness uncertainty related scale uncertainties will be substantially reduced if the positron and electron data are recorded with the same targets. Using electron data from E12-06-104, E12-24-001, and E12-14-002 to form the ratios is a fallback that we have built in, but is not the ideal run condition.

The proposal laid out here assumes that we begin the experiment with one lepton beam (be that electrons or positrons), complete all data that uses that beam type, and then reconfigure to the other lepton beam to record the remaining data. As each beam type and energy involves many different spectrometer kinematics, changing between beam types more frequently does not confer any improvement to our data. To be clear, this condition *does not* require multiple machine reconfigurations between electrons and positrons, but rather that a single reconfiguration occurs such that data is recorded on the same targets. That being said, so long as we run at each beam type and energy for long enough that we do not have to return to the configuration more than once, the data will not be harmed by going between electrons and positrons more than once if it aids in scheduling.

2.3 Statistics and Systematics

The systematic uncertainties related to the extraction of two-photon effects in SIDIS and DIS are similar, although not identical, to those in the extraction of effects due to Coulomb Corrections. In the sections below, we will address significant sources of uncertainty.

2.3.1 Kinematics and Acceptance

A key advantage of using moderate-acceptance, magnetic-focusing spectrometers is that the acceptance for positively and negatively charged particles is identical. Assuming the same parent distributions, the family of particle trajectories in the HMS and SHMS detector huts will be the same for electrons and positrons. In the case of the inclusive DIS measurements, we are comparing electrons and positrons recorded in the same spectrometer. We conservatively assume a 0.1% systematic uncertainty in the e^+/e^- ratios due to the description of the acceptance. This 0.1% allows for some uncertainty due to possible variations in the event distributions.

In the case of the SIDIS measurements, we are comparing electrons to positrons in the HMS, while the SHMS stays at fixed polarity (i.e. π^+ or π^-). We assign a (conservative) uncertainty of 0.1% in each arm in the positron to electron ratios yielding a total contribution of 0.14% to the cross section ratios.

For the Coulomb Corrections studies, we compare the super–ratio of $\frac{(\sigma_A/\sigma_H)^{e^+}}{(\sigma_A/\sigma_H)^{e^-}}$. In the A/D ratio, there is some systematic uncertainty associated with the difference in acceptance for thin, solid targets and extended (10 cm long) cryotargets. In the super–ratio, this contribution cancels, and the only remaining contribution comes from possible differences in the event distributions, leading to a total uncertainty of 0.2%.

In both the direct e^+/e^- cross section ratios from LH2 and LD2 and the A/D target super-ratios, uncertainties due to kinematics are also expected to be quite small. Studies from E12-10-008 [39] show that the contribution from global kinematic offsets contribute less than 0.1% in the DIS regime when taking the cross section ratio of targets at the same time. Another contribution that will be relevant in this experiment is the reproducibility of kinematic settings when data are taken in two different time periods, as will be the case for the e^+/e^- cross section ratios for LH2 and LD2. While the absolute beam energy can be measured to a precision of $\delta E/E$ of 5×10^{-4}, the relative energy can be tracked using the so-called Tiefenback energy to about 1 MeV. The knowledge of absolute value of the central momentum of the Hall C spectrometers is of the order 1×10^{-3}, the reproducibility of the spectrometers momentum setting is of the order $2 - 3 \times 10^{-4}$. Both of these contributions are significantly smaller than a 0.1% effect on the cross section (and therefore the ratio). The central angles of the spectrometers are reproducible to about 0.2 mrad, which results in a 0.15% to 0.46% variation in the DIS and SIDIS cross sections. This will contribute directly to the e^+/e^- cross section ratios for the cryogenic targets.

2.3.2 Beam current measurement

The beam current in Hall C is typically measured using the combination of the hall BCMs and the Unser monitor to provide an absolute calibration. The absolute uncertainty in the beam current measurement using this technique is dominated by the 200 nA noise in the Unser. At beam currents of 20-30 μA, this results in absolute uncertainties of 0.7–1%.

For the lower current (1 μA) positron beam, the Unser cannot be used to provide the absolute calibration. Rather, one can calibrate the hall BCMs relative to the Faraday cup in the injector. This calibration assumes no or minimal beam loss between the injector and Hall C, so will have a somewhat larger uncertainty. We assume a relative uncertainty of about 2% (similar to that achieved during the Q-Weak experiment [40]) will be achievable.

The absolute BCM calibration will result in a normalization (or scale) uncertainty when forming the e^+/e^- ratios. In this case, we are also concerned about potential point-to-point, or ε dependent uncertainties. Since there are several BCMs in Hall C (5), the time-dependence can be monitored by comparing different pairs of BCMs. This was done for E12-10-008, and an uncertainty of 0.35% was assigned due to these variations. We assume that we can achieve similar precision during this experiment.

The scale uncertainty for measuring the positron beam current is the largest contribution to the total scale uncertainty in the TPE studies. As stated above, this is due to the lack of a device in the hall beamline capable of measuring low currents accurately for an absolute calibration. There have been discussions regarding the development of such a device, such as a Faraday cup in Hall C. While none of these discussions have been concrete enough to make us feel that it is fair to assume an improved uncertainty at the time of writing, we hope that these discussions will continue and lead to a positron beam current measurement of 1% or better.

For the Coulomb Correction measurements, only the point-to-point uncertainty applies since one will be comparing electron A/H ratios to positron ratios.

2.3.3 Target Cell Background

The 10 cm hydrogen target cell has aluminum walls that will contribute a background to this measurement. In order to characterize and subtract this contribution, we will include an empty target cell to measure the contribution from the cell. We plan to allocate additional time to this equivalent to 20% of the beam time used on the hydrogen target. Measurement of this background should contribute negligible systematic uncertainty since identical targets will be used for electron and positron running.

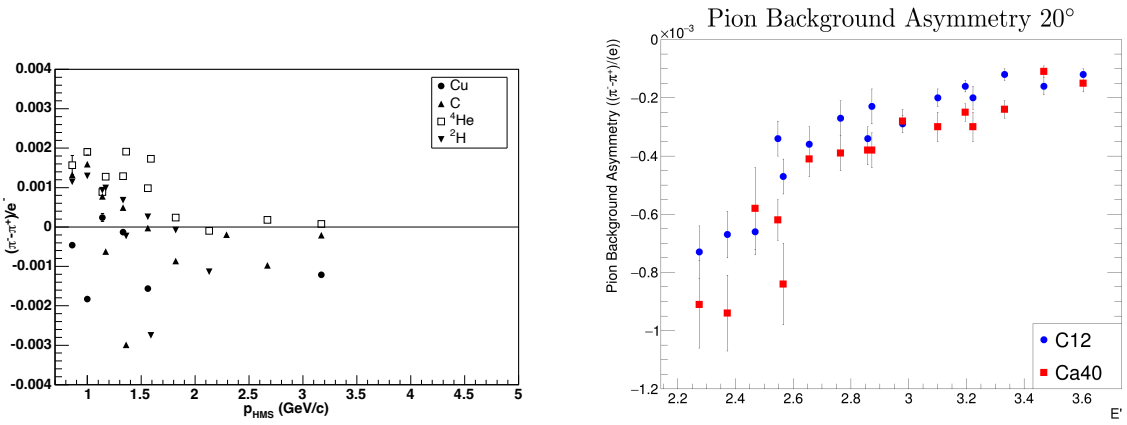

Figure 20: *Left:* Measurement of the difference in charged pion yield ($\pi^- - \pi^+$)) relative to the electron yield from experiment E03-103 [41]. Data were taken at $E_{beam} = 5.77$ GeV with the HMS at 40°. *Right:* Difference in charged pion yield relative to electron yield from E12-10-008 [42]. Data were taken at 10.5 GeV with the HMS at 20°.

2.3.4 Charge Symmetric Background

A common background source for inclusive scattering is charge symmetric background (CSB). This background is excess detection of electrons (positrons) due to pair production processes, most commonly π^0 decay to a photon pair followed by the subsequent production of an e^+e^- pair from one of the photons. This has been found to be a significant background source for inclusive DIS, though it has been found to be largely insignificant in SIDIS data [2]. The data necessary for parameterizing CSB will be collected during the experiments E12-06-104, E12-14-002, and E12-24-001. The π^0 production cross section does not change between an electron and a positron beam which allows us to use these past data for characterizing and subtracting our background for both beam species.

2.3.5 Pion backgrounds

Pions are rejected in the Hall C spectrometers using a combination of their lead-glass calorimeters and threshold gas Cherenkov detectors. In the analysis of electron data in Hall C, one can empirically measure the amount of pion contamination that remains after applying appropriate particle ID constraints by studying "open trigger" data that includes a significant pion sample. In most cases, it turns out that the π^+ and π^- inclusive cross sections are similar enough that in the act of subtraction the charge symmetric background (which will include some contamination from inclusive π^+) we are also subtracting any residual pion contamination.

The effectiveness of this subtraction is illustrated in the figure below 20. The plots show the difference in charged pion yield ($\pi^- - \pi^+$) compared to the electron yield. The plot on the left is from the E03-103 ($E_{beam} \approx 6$ GeV) data in Hall C, while the plot on the right is from the recent E12-10-008, 12 GeV experiment. In both cases, the charged pion difference is only a small fraction when compared to the electron yield (at most 0.2% at small momentum, low energy) yielding a small systematic uncertainty in the resulting pion contamination. Since the positron inclusive cross sections are expected to be similar to the electron cross section, the pion contamination effects will be similar. We assume a 0.2% point-to-point uncertainty in electron-positron cross section ratios, and similar for the CC target ratios.

2.3.6 Radiative Corrections

This experiment will attempt to glean information about possible contributions from hard two-photon exchange via the measurement of cross section ratios. Since the primary observable is the ratio of cross sections from the same target (or pair of targets), the only notable source of uncertainty due to conventional radiative cross sections is that from the *difference* in radiative corrections between the

two measurements.

For the ratio of e^+ to e^- cross sections, since the same targets will be used, the only source of uncertainty in the difference of radiative cross sections will come from possible differences in the Born cross section leading to different corrections. Even with effects from hard two-photon exchange, the e^+ and e^- cross sections will be similar enough that this contribution should be small. We assign a (conservative) uncertainty of 0.5% to the difference in radiative corrections between the e^+ and e^- cross sections.

For the study of Coulomb Corrections, similar considerations apply. While the A/D ratio itself may have somewhat large radiative correction uncertainties, the A/D super-ratio will have small uncertainty on the difference in radiative corrections. We again assume 0.5% for the uncertainty in this observable.

2.3.7 Target boiling

The positron data will be taken at very low currents, so the impact of target heating due to the positron beam will be small. However, the electron data will be taken at higher currents, of the order 25 μA. The density reduction of standard Hall C cryotargets has been measured to be $\approx 2.5 \pm 0.3\%/100\mu A$. At the nominal electron current planned for this experiment, this translates to an uncertainty of about 0.1% on the effective target thickness.

The systematic uncertainties for the two-photon and Coulomb Correction measurements are summarized in Tables 1 and 2. The point-to-point systematic uncertainties for each case are ∼0.5%, while the scale uncertainties are 2.1% for the two-photon measurements and 0.56% for the Coulomb Corrections.

Source	$\delta R/R$ (%) point-to-point	$\delta R/R$ (%) scale
Spectrometer momentum	-	$< 0.1\%$
Beam energy	-	$< 0.1\%$
θ_{spec}	0.15-0.46%	$< 0.1\%$
Charge	0.35%	2%
Target Boiling	-	0.1%
Total dead time	0.15%	0.14%
Detector efficiency	0.11%	-
Charge Symmetric Background	-	-
Pion background	0.2%	-
Radiative Corrections	-	0.5%
Acceptance	0.1-0.14%	-
Cryotarget wall subtraction	-	-
Total	0.48-0.65%	2.07%

Table 1: Projected systematic uncertainties for measurement of the e^+/e^- cross section ratios for inclusive and semi-inclusive DIS. Uncertainties are broken into point-to-point and overall scale contributions. Uncertainties are based on those achieved in previous Hall C experiments, with modifications to account for the unique positron running conditions.

2.4 Kinematics

While the impact of these proposed data would be maximized by studying TPE for SIDIS at all of the kinematics of E12-06-104 and for DIS at all of the kinematics of E12-14-002, we have opted to propose this experiment using a tailored subset of these kinematics in recognition of the substantial beam time request the alternative would require. The details of the choice of this subset are discussed below.

2.4.1 SIDIS

In the interest of time, we plan to use two triggers, coincidence and HMS single-arm, to record both DIS and SIDIS data at the same time. As SIDIS is a much lower rate reaction, the DIS data uncertainties will be dominated by systematics with very little statistical uncertainty contribution. The kinematics

Source	$\delta R/R$ (%) point-to-point	$\delta R/R$ (%) scale
Spectrometer momentum	-	$< 0.1\%$
Beam energy	-	$< 0.1\%$
θ_{spec}	-	$< 0.1\%$
Charge	0.35%	-
Target Boiling	-	0.1%
Total dead time	0.15%	0.14%
Detector efficiency	0.11%	-
Charge Symmetric Background	-	-
Pion background	0.2%	-
Radiative Corrections	-	0.5%
Acceptance	0.2%	-
Cryotarget wall subtraction	-	-
Total	0.49%	0.56%

Table 2: Projected systematic uncertainties for measurement of the super-ratio, $\frac{(\sigma_A/\sigma_H)^{e^+}}{(\sigma_A/\sigma_H)^{e^-}}$. Uncertainties are broken into point-to-point and overall scale contributions. Uncertainties are based on those achieved in previous Hall C experiments, with modifications to account for the unique positron running conditions.

				HMS		SHMS	
x	Q^2	E_0	z	$E_{e'}$	$\theta_{e'}$	E_π	θ_π
0.25	3.3	8.6	0.36	1.6	28.7°	2.6	7.9°
			0.5	1.6	28.7°	3.6	7.9°
			0.67	1.6	28.7°	4.9	7.9°
0.25	3.3	10.7	0.36	3.7	16.7°	2.6	10.3°
			0.5	3.7	16.7°	3.6	10.3°
			0.67	3.7	16.7°	4.9	10.3°
0.31	3.1	6.5	0.5	1.1	37.7°	2.8	9.2°
		8.6	0.5	3.3	19.2°	2.8	13°
		10.7	0.5	5.4	13.4°	2.8	14.7°

Table 3: The kinematic and spectrometer settings for SIDIS TPE studies. The HMS will be set to detect the scattered beam lepton. The SHMS will be set to detect the final hadronic state pion. For all kinematics, $\theta_{\pi q} = 2°$. All kinematics will be recorded with a π^+ in the final state. The three data points at $x = 0.31$ and $Q^2 = 3.1$ GeV^2 will also be recorded for a π^- final state. All lepton kinematics will be simultaneously recorded with an inclusive trigger in the HMS for the DIS TPE studies.

selected are listed in Table 3. These kinematics are the same for the SIDIS TPE and CC studies, with the exception of the z scan at $x = 0.25$, $Q^2 = 3.3$ and the π^- measurements which will be omitted for CC studies.

2.4.2 Inclusive DIS

By using a coincidence (SIDIS) and singles (inclusive) triggers, a portion of the inclusive data collection will not add additional time to the total amount of beam time. Additionally, since the SIDIS event rate is smaller than the inclusive, this ensures sufficient statistical precision for the kinematics. Along with these overlapping kinematics, we will also make measurements at two additional settings. These will allow for the investigation of possible x and Q^2 TPE effects. At these settings, we will match the precision of the E12-14-002 experiment. The full kinematic coverage is enumerated in Table 4 and shown in Figure 21.

x	Q^2	E_0	ε	$E_{e'}$	$\theta_{e'}$
0.25	3.3	8.6	0.32	1.6	28.7°
		10.7	0.59	3.7	16.7°
0.31	3.1	6.5	0.3	1.1	37.7°
		8.6	0.63	3.3	19.2°
		10.7	0.78	5.4	13.4°
0.1	1	6.5	0.34	1.2	20.9°
		8.6	0.66	3.3	10.8°
		10.7	0.8	5.4	7.6°
0.225	1.9	5.5	0.33	1	34.2°
		6.5	0.55	2	22°
		8.6	0.77	4.1	13.3°
		10.7	0.87	6.2	9.7°
0.3	1.9	4.4	0.41	1	37.9°
		5.5	0.66	2.1	23.3°
		6.5	0.78	3.1	17.6°
		8.6	0.89	5.2	11.8°
0.3	3	6.5	0.33	1.2	36.6°
		8.6	0.66	3.3	18.8°
		10.7	0.8	5.4	13.1°
0.4	3	5.5	0.48	1.5	35.1°
		6.5	0.66	2.5	24.8°
		8.6	0.83	4.6	15.8°
		10.7	0.9	6.7	11.7°
0.5	3	4.4	0.47	1.2	44.2°
		5.5	0.7	2.3	28.2°
		6.5	0.8	3.3	21.5°
		8.6	0.9	5.4	14.6°
		10.7	0.94	7.5	11.1°
0.5	5	6.5	0.31	1.2	47.8°
		8.6	0.65	3.3	24.3°
		10.7	0.8	5.4	17°
0.6	5	5.5	0.32	1.1	55.2°
		6.5	0.55	2.1	35.6°
		8.6	0.78	4.2	21.6°
		10.7	0.87	6.3	15.7°

Table 4: Kinematics for DIS TPE studies. The first two x, Q^2 entries are taken simultaneously with the SIDIS TPE data. The rest are recorded separately with $x = 0.5$ and above in the HMS and below $x = 0.5$ in the SHMS.

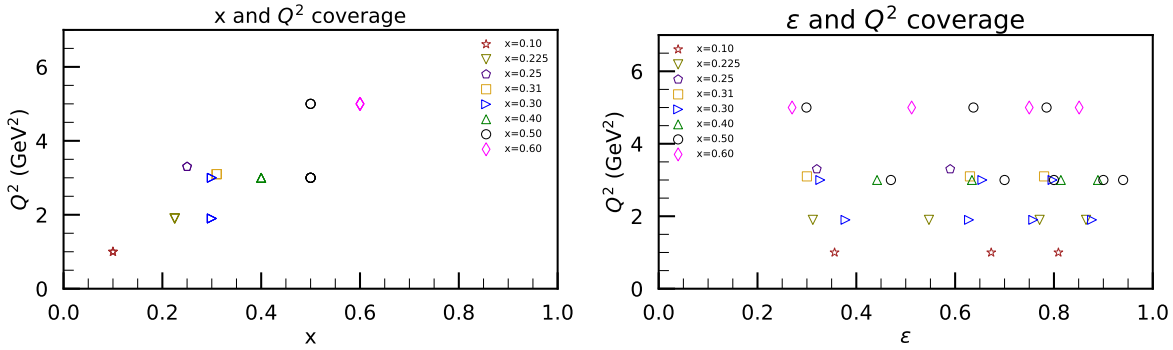

Figure 21: Kinematic coverage for TPE studies in inclusive DIS.

					Times (hrs)			
x	Q^2	E_0	ε	z	π^+, e^+	π^+, e^-	π^-, e^+	π^-, e^-
0.25	3.3	8.6	0.32	0.36	49.4	2		
				0.5	36.4	1.5		
				0.67	37.8	1.5		
0.25	3.3	10.7	0.59	0.36	6.3	1		
				0.5	4.7	1		
				0.67	5	1		
0.31	3.1	6.5	0.3	0.5	105.8	4.2	252.5	10.1
		8.6	0.63	0.5	8.6	1	20.1	1
		10.7	0.78	0.5	2.3	1	5.3	1
Totals					256.3	14.2	277.9	12.1

Table 5: Kinematics and time request for studies of two-photon exchange in SIDIS. The four time columns have headers that show the hadronic final state detected in the SHMS followed by the lepton beam type. All times were calculated for a 10k statistics goal. Times using a positron beam assume a current of 1 μA. Times using an electron beam assume 25 μA. Particularly short electron beam times have been rounded up to require a minimum of 1 hour at each setting. These kinematics include two x, Q^2 points and a z scan at the $x = 0.25$, $Q^2 = 3.3$ as is planned for E12-06-104 [2]. All kinematics above have $\theta_{\pi q} = 2^\circ$.

3 Beamtime Request

3.1 SIDIS Two-Photon Exchange

Table 5 enumerates the kinematics and beam time request for the SIDIS TPE measurements. This includes two x, Q^2 points as well as a z-scan at $x = 0.25$, $Q^2 = 3.3$. All kinematics will record data with a π^+ in the final state. We will also record data with a π^- in the final state at the $x = 0.31$, $Q^2 = 3.1$ kinematic. These data will be recorded using the 10cm hydrogen target. To achieve a 1% statistical uncertainty, we aim to collect 10k SIDIS events at each kinematic. Our projections for these results are shown in Fig. 22 using TPE predictions extracted from Fig. 10. Note that the kinematics of the prediction and our projections are close, but not identical. Our kinematics are at a higher Q^2 than the predictions and it is expected that TPE will increase with Q^2. In all, these data will allow us to study whether TPE in SIDIS is different from TPE in DIS, dependent on z, and dependent on the hadronic final state.

3.2 Inclusive DIS

Inclusive DIS data for TPE will be recorded at the same time as the SIDIS TPE data to get two data points. However, by not selecting a specific hadronic final state, DIS data can be recorded much more rapidly than SIDIS. For that reason, we have opted to include a larger subset of data for DIS that will not be taken at the same time as SIDIS, which would require a prohibitively large amount of

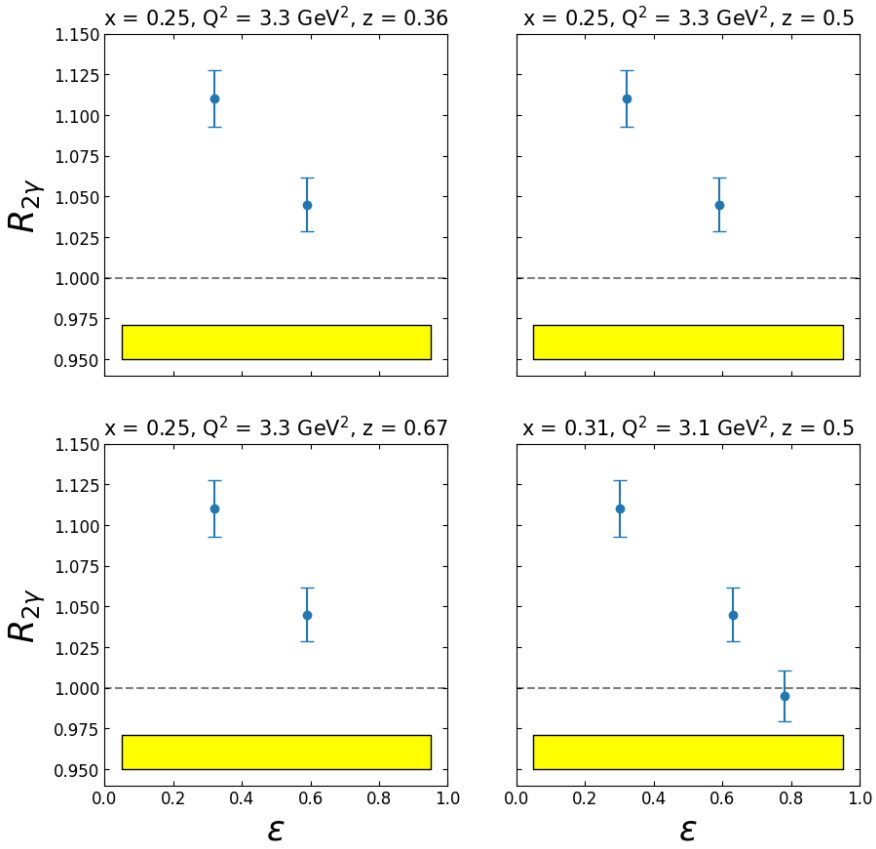

Figure 22: Projections for the SIDIS TPE measurements. These figures include a 1% statistical uncertainty in each cross section and projected systematic uncertainties from Table 1. The yellow-band shows the normalization uncertainty of 2.07% anticipated from recording positron and electron data in the same run period.

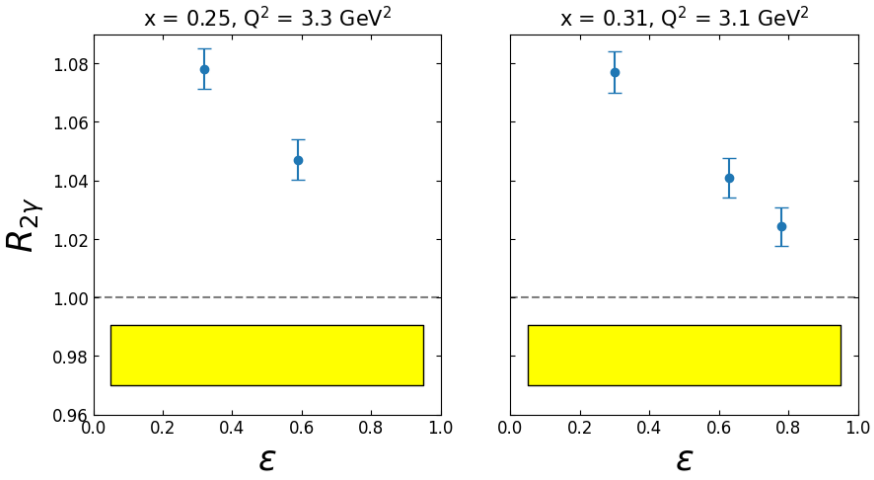

Figure 23: Projections for the DIS TPE measurements. These figures include projected systematic uncertainties from Table 1 and projected statistical uncertainties. As these data are higher rate than SIDIS and recorded concurrently, the statistical uncertainties are negligible. The yellow-band shows the normalization uncertainty of 2.07% anticipated from recording positron and electron data in the same run period.

time to achieve useful statistics. For this, we have selected additional data points from the E12-14-002 experiment [4] that allow us to cover a large range in x, from 0.1 to 0.6, and at a variety of Q^2 values, from 1 to 5 GeV^2 with a few Q^2 values having multiple x measurements to assess the x dependence of TPE effects.

As the SHMS will not be used for SIDIS pions during these measurements, we will divide the kinematics between the two spectrometers so that multiple kinematics can be studied at once. For this, we have chosen all data points at $x = 0.5$ and $x = 0.6$ to be in the HMS as they are lower rate and the HMS has a larger solid angle. All other kinematics will be studied in the SHMS. This is not a strictly 50/50 division going by raw hours required, but it ensures that each spectrometer has a kinematic at each beam energy (that is, if we only put the two highest Q^2 kinematics in the HMS it would not have any measurements during the beam time at 4.4 GeV) and that the lower rate kinematics can be completed successfully. As such, though the lower x kinematics do not need the full time we will devote to the higher x kinematics, they will instead benefit from increased statistics. This is a benefit as the TPE effects are predicted to be smaller at the lower x kinematics.

Projections for the kinematics recorded simultaneously with the SIDIS data are shown in Fig. 23. As the SIDIS rate as substantially lower than the DIS rate, the statistical uncertainties on these data are negligible. Projections for the kinematics recorded independently are shown in Fig. 24. The beam time requests were initially determined with a goal of 1% statistical uncertainty in each of the e^+ and e^- measurements. These uncertainties have been improved due to rounding and, particularly in the case of e^- measurements, a requirement that each kinematic be recorded for a minimum of an hour. The statistical uncertainties in these projections reflect the anticipated total statistics based on the times listed in Table 6. While we have noted above that there will also be some further statistical improvement due to the way we have divided the time between the two spectrometers, we have not included that in these figures.

The magnitude of TPE effects in both figures are calculated using a prescription a prescription from Ref. [43],

$$\delta_{2\gamma} = -0.069\,(1-\varepsilon)\ln\left(0.394\text{GeV}^{-2}Q^2+1\right). \tag{16}$$

This equation is based on a fit to world elastic data and assumes the full form factor discrepancy is attributable to "hard" TPE. The fit also assumes that there is a Q^2 dependent piece that incorporates quark degrees of freedom for high Q^2 scattering. We have opted to use this fit in the absence of *any* available calculations for TPE in DIS.

				SHMS Time (hrs)		HMS Time (hrs)	
x	Q^2	E_0	ε	e^+	e^-	e^+	e^-
0.1	1	6.5	0.34	1	1		
		8.6	0.66	1	1		
		10.7	0.8	1	1		
0.225	1.9	5.5	0.33	1	1		
		6.5	0.55	1	1		
		8.6	0.77	1	1		
		10.7	0.87	1	1		
0.3	1.9	4.4	0.38	1	1		
		5.5	0.63	1	1		
		6.5	0.76	1	1		
		8.6	0.88	1	1		
0.3	3	6.5	0.33	1	1		
		8.6	0.66	1	1		
		10.7	0.8	1	1		
0.4	3	5.5	0.44	2	1		
		6.6	0.63	1	1		
		8.6	0.81	1	1		
		10.7	0.89	1	1		
0.5	3	4.4	0.47			5	1
		5.5	0.7			2	1
		6.6	0.8			1	1
		8.8	0.9			1	1
0.5	5	6.6	0.3			16	1
		8.8	0.64			4	1
		11	0.79			3	1
0.6	5	5.5	0.27			20	1
		6.6	0.51			6	1
		8.8	0.75			3	1
		10.7	0.85			2	1
Totals				19	18	63	11

Table 6: Kinematics for Two Photon Exchange studies in inclusive Deep Inelastic Scattering. The two x, Q^2 settings in Table 5 will also have DIS TPE data but are omitted here as they do not require additional beam time beyond the time required for the SIDIS TPE data. The kinematics here cannot be recorded concurrently with the SIDIS data and thus require additional beam time. Kinematics at $x = 0.5$ and above will be recorded in the HMS and kinematics below $x = 0.5$ will be recorded in the SHMS. For the positron beam, the HMS time drives the beam time request. For the electron beam, the SHMS time drives the beam time request. These times were chosen to achieve 1% statistical uncertainty and then adjusted to so that no setting was shorter than 1 hour.

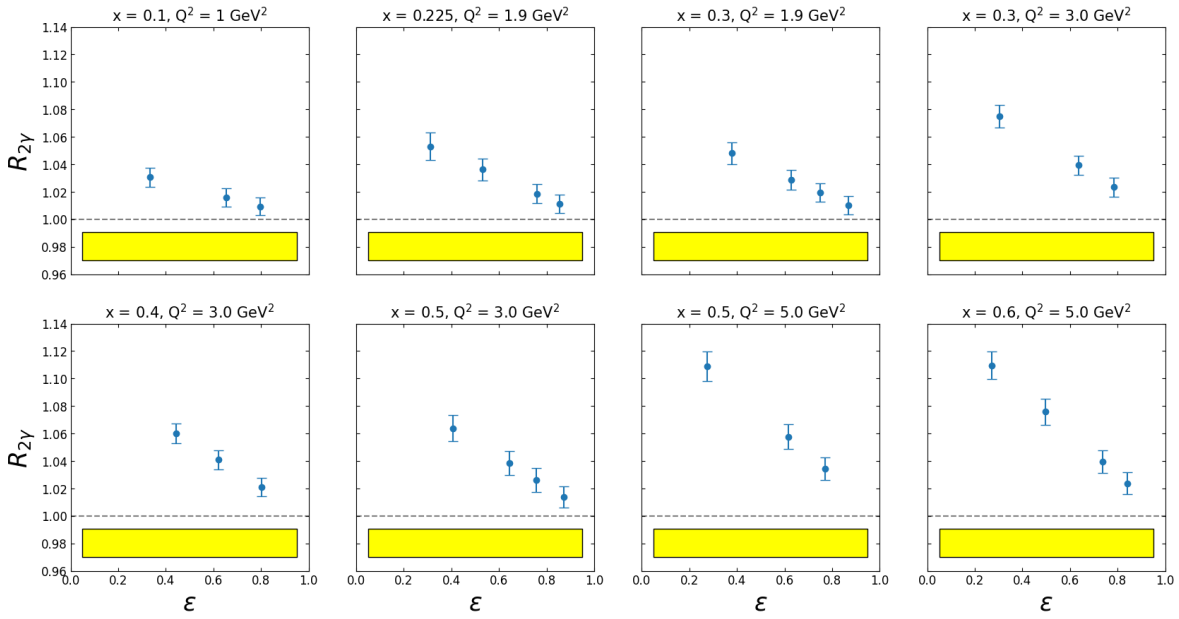

Figure 24: Projections for the non-concurrent DIS TPE measurements. These figures include projected systematic uncertainties from Table 1 and the projected statistical uncertainties in each cross section measurement. These data will allow for characterization of the Q^2 and x dependence of TPE effects in inclusive DIS. The yellow-band shows the normalization uncertainty of 2.07% anticipated from recording positron and electron data in the same run period.

3.3 SIDIS Coulomb Corrections

The data on the copper target for the study of Coulomb Corrections cannot be recorded in tandem with the other studies as it requires a different target. However, the hydrogen data necessary is the same data needed for the SIDIS TPE studies and does not require additional time. In table 7, we summarize the kinematics and beam time request for this study. The times in the table are *only* for the copper target since the hydrogen data is already accounted for. The Coulomb Corrections kinematics are identical to the SIDIS TPE kinematics with the omission of the z-scan and the π^- data. That is, the SHMS will be set to detect π^+ with $z = 0.5$ and $\theta_{pq} = 2°$. Projected results, assuming the IEMA is valid, are shown in Figure 25.

				Times (hrs)	
x	Q^2 (GeV^2)	E_0 (GeV)	ε	e^+	e^-
0.25	3.3	8.6	0.60	88.5	3.5
		10.7	0.33	11.5	1
0.31	3.1	6.5	0.30	252.6	10.1
		8.6	0.63	21.8	1
		10.7	0.78	5.8	1
Totals				380.2	16.6

Table 7: Kinematics and beam time requests for Coulomb Correction studies. These studies are all done at $z = 0.5$. The times included in this table *only* include the time needed for the copper target. The hydrogen data required to form the double ratio are the same as the data that is planned for SIDIS TPE, so that time is already included in Table 5. The e^+ time column assumes a 1 μA positron beam. The e^- time column assumes a 25 μA electron beam. The electron beam times have been adjusted to require a minimum of 1 hour at each setting.

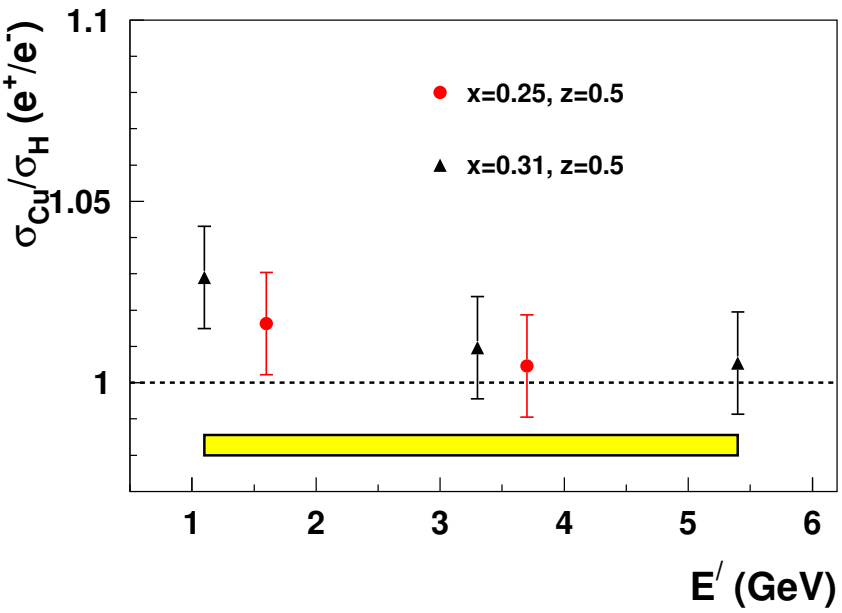

Figure 25: Projections for the measurement of the super-ratio, $\frac{(\sigma_A/\sigma_H)^{e^+}}{(\sigma_A/\sigma_H)^{e^-}}$. The yellow band indicates the 1σ normalization uncertainty, while the error bars on the points include statistical (1% in each cross section measurement) and point-to-point systematic uncertainties combined in quadrature. The systematic uncertainties included are enumerated in Table 2.

3.4 Total Request and Overhead

Table 8 summarizes the total beam time request of this proposal. Included are the times needed for production data, as well as activities related to kinematic and target changes, pass changes, and background studies. We assume 1 hour per kinematic change, 15 minutes for target changes, and 8 hours (one shift) for each pass change. Kinematic changes include angle and momentum changes for either or both spectrometers. This table include the production time and overhead for both the positron and electron measurements. Note that the time to switch the beam from positrons to electrons is not included.

As previously stated, the times assume a 1 μA positron beam and a 25 μA electron beam. The calculated times were set to achieve 1% statistical uncertainty on each cross section point. If higher currents are available (particularly for the positron beam), we would aim to use that in order to achieve higher statistical precision.

4 Experiments with similar or related goals

There are no other experiments that aim to study the same physics as this proposal. That being said, there are several planned JLab experiments that are highly related and complimentary to this measurement. Below, we discuss the goals and techniques of these experiments and how they differ from this proposal.

4.1 Single Spin Asymmetry Experiments

An approved experiment, E12-22-004 [44], will measure the beam normal single spin asymmetry for DIS using the future SoLID spectrometer. This will provide the first precision measurement of the asymmetry in DIS and will complement future target normal single spin asymmetry measurements. This asymmetry is sensitive to the imaginary component of the TPE amplitude.

Activity	e^+ Time (hrs)	e^- Time (hrs)
TPE π^+ Production	256.3	14.2
TPE π^- Production	277.9	12.1
CC Production	380.2	16.6
Dedicated DIS Production	63	18
Pass Changes	40	40
Kinematic Changes	38	38
Target Changes	21	21
Empty Target	119.4	8.9
Target Boiling Studies	4	4
BCM Calibrations	8	8
Detector Checkout	12	
Subtotals	1219.8	180.8
Total	1400.6 hours	(58.4 days)

Table 8: Total time request broken down by activity and beam type

Additionally a run group experiment with SoLID [45] with measure the target normal single spin asymmetries for DIS using a transversely polarized ^{3}He and NH_3 target, allowing to measure the asymmetry for both protons and neutrons.

4.2 JLab Elastic Two Photon Exchange Experiments

JLab E12+23-008 [46] will study TPE in the elastic regime using the CLAS12 spectrometer using a similar technique to this proposal. This experiment will record coincident $e^+ - p$ and $e^- - p$ events in order to form an $R_{2\gamma} = e^+/e^-$ ratio for a wide Q^2 range.

JLab E12+23-012 [14] will study TPE in the elastic regime using the HMS in Hall C to perform Super Rosenbluth extractions. This experiment will detect the recoil proton which is less susceptible to uncertainties arising from the beam energy and spectrometer angle.

4.3 Inelastic R_{LT} Experiments

As discussed in Section 1.4, there are three upcoming experiments in Hall C that will study R_{LT} in SIDIS (E12-06-104 [2]), in nuclear SIDIS (E12-24-001 [3]), and in inclusive DIS (E12-14-002 [4]). These experiments are highly related to our proposal in that we aim to mirror many of their kinematics so that our results may have maximal impact on their results. Specifically, TPE and CC, if sizable, are able to meaningfully change the physics interpretations of these results. This aspect of their analysis cannot be assessed without this proposed measurement.

4.4 DIS Coulomb Corrections Experiment

JLab E12+23-003 [1] will study Coulomb Corrections in inclusive DIS. The technique used is identical to ours (i.e. e^+/e^- super ratio with a nuclear target), but is does not study SIDIS. We believe that this experiment and ours are highly complimentary in that it is critical to understand CCs in both scattering regimes. Additionally, it is an open question if CCs are the same in DIS and SIDIS.

5 Summary

This proposal aims to use the planned CEBAF positron upgrade (Ce^+BAF) to study two-photon exchange in inclusive and semi-inclusive deep inelastic scattering and Coulomb Corrections in semi-inclusive deep inelastic scattering. These processes are nearly completely unmeasured and unconstrained and may have a significant impact on the interpretation of past and future JLab data. Of particular note, if these effects are sizable, they can dramatically change the results of upcoming LT separation measurements. The opportunity to measure this with Ce^+BAF will have wide-ranging impact for JLab data and beyond.

References

[1] D. Gaskell, N. Fomin, and W. Henry. spokespersons, Jefferson lab experiment C12+23-003, 2023.

[2] R. Ent and H. Mkrtchyan. spokespersons, Jefferson lab experiment E12-06-104, 2006.

[3] P. Bosted, W. Brooks, R. Ent, D. Gaskell, E. Kinney, and H. Mkrtchyan. spokespersons, Jefferson lab experiment E12-24-001, 2024.

[4] S. Alsalmi, M. E. Christy, D. Gaskell, T. J. Hague, W. Henry, S. Malace, D. Nguyen, and P. Solvignon-Slifer. spokespersons, Jefferson lab experiment E12-14-002 jeapardy update, 2023.

[5] M. K. Jones et al. 84:1398, 2000.

[6] A. J. R. Puckett et al. Recoil Polarization Measurements of the Proton Electromagnetic Form Factor Ratio to $Q^2 = 8.5$ GeV^2. *Phys. Rev. Lett.*, 104:242301, 2010.

[7] I. A. Rachek et al. Measurement of the two-photon exchange contribution to the elastic $e^{\pm}p$ scattering cross sections at the VEPP-3 storage ring. *Phys. Rev. Lett.*, 114:062005, 2015.

[8] D. Rimal et al. Measurement of two-photon exchange effect by comparing elastic $e^{\pm}p$ cross sections. *Phys. Rev. C*, 95:065201, 2017.

[9] B. S. Henderson et al. Hard Two-Photon Contribution to Elastic Lepton-Proton Scattering: Determined by the OLYMPUS Experiment. *Phys. Rev. Lett.*, 118:092501, 2017.

[10] Joshua Ellis. TikZ-Feynman: Feynman diagrams with TikZ. *Comput. Phys. Commun.*, 210:103–123, 2017.

[11] P. G. Blunden and W. Melnitchouk. Dispersive approach to two-photon exchange in elastic electron-proton scattering. *Phys. Rev. C*, 95:065209, 2017.

[12] Nikolai Kivel and Marc Vanderhaeghen. Two-photon exchange in elastic electron-proton scattering: QCD factorization approach. *Phys. Rev. Lett.*, 103:092004, 2009.

[13] E. A. Kuraev, V. V. Bytev, S. Bakmaev, and E. Tomasi-Gustafsson. Charge asymmetry for electron (positron)-proton elastic scattering at large angle. *Phys. Rev. C*, 78:015205, 2008.

[14] J. Arrington, M. Nycz, , S. N.Santiesteban, and M.Yurov. spokespersons, Jefferson lab experiment E12+23-012 proposal, 2023.

[15] H. Jöstlein, I.J. Kim, K. Königsman, A.C. Melissinos, P. Mühlemann, E. Aslanides, and P. Limon. Two-photon exchange in deep inelastic scattering. *Physics Letters B*, 52(4):485–488, 1974.

[16] A. Airapetian et al. Search for a Two-Photon Exchange Contribution to Inclusive Deep-Inelastic Scattering. *Phys. Lett. B*, 682:351–354, 2010.

[17] J. Katich et al. Measurement of the Target-Normal Single-Spin Asymmetry in Deep-Inelastic Scattering from the Reaction $^3\mathrm{He}^{\uparrow}(e,e')X$. *Phys. Rev. Lett.*, 113(2):022502, 2014.

[18] S Lee, A Afanasev, and H Avakian. Two-photon exchange for semi-inclusive meson production. `https://indico.jlab.org/event/819/contributions/14212/attachments/10815/16583/Positron_Working_Workshop_Slides__2024_.pdf`, 2024.

[19] Stinson Lee and Andrei Afanasev. Soft-Photon Contribution into Two-Photon Exchange Corrections for Azimuthal Asymmetries of SIDIS. 4 2025.

[20] Patricia Solvignon, Dave Gaskell, and John Arrington. Coulomb Distortion in the Inelastic Regime. *AIP Conf. Proc.*, 1160(1):155–159, 2009.

[21] E. Calva-Tellez and D. R. Yennie. Coulomb Corrections to Deep Inelastic Electron or Muon Scattering From Nuclei. *Phys. Rev. D*, 20:105, 1979.

[22] P. Gueye et al. Coulomb distortion measurements by comparing electron and positron quasielastic scattering off C-12 and Pb-208. *Phys. Rev. C*, 60:044308, 1999.

[23] Jörn Knoll. An analytic description of inelastic electron scattering on nuclei. *Nucl. Phys. A*, 223:462–476, 1974.

[24] M. Traini and M. Covi. Quasielastic electron scattering off nuclei: A Study of Coulomb distortion effects. *Nuovo Cim. A*, 108:723–736, 1995.

[25] M. Traini. Separation of longitudinal and transverse structure functions in (e,e-prime) quasielastic scattering off nuclei including Coulomb corrections. *Nuovo Cim. A*, 108:1259–1267, 1995.

[26] Andreas Aste, Cyrill von Arx, and Dirk Trautmann. Coulomb distortion of relativistic electrons in the nuclear electrostatic field. *Eur. Phys. J. A*, 26:167–178, 2005.

[27] S. Dasu et al. Measurement of kinematic and nuclear dependence of $r = \frac{\sigma_L}{\sigma_T}$ in deep inelastic electron scattering. *Phys. Rev. D*, 49:5641–5670, Jun 1994.

[28] V. Tvaskis et al. Longitudinal-transverse separations of deep-inelastic structure functions at low Q^2 for hydrogen and deuterium. *Phys. Rev. Lett.*, 98:142301, Apr 2007.

[29] L.H. Tao et al. Precision measurement of $r = \frac{\sigma_L}{\sigma_T}$ on hydrogen, deuterium, and beryllium targets in deep inelastic electron scattering. *Z. Phys. C*, 70, 1996.

[30] C. J. Bebek, C. N. Brown, M. Herzlinger, S. D. Holmes, C. A. Lichtenstein, F. M. Pipkin, S. Raither, and L. K. Sisterson. Scaling behavior of inclusive pion electroproduction. *Phys. Rev. Lett.*, 34:759–761, Mar 1975.

[31] C. J. Bebek, A. Browman, C. N. Brown, K. M. Hanson, R. V. Kline, D. Larson, F. M. Pipkin, S. W. Raither, A. Silverman, and L. K. Sisterson. Longitudinal-transverse separation for inclusive electroproduction of pions and protons. *Phys. Rev. Lett.*, 38:1051–1054, May 1977.

[32] C. J. Bebek, C. N. Brown, M. S. Herzlinger, S. D. Holmes, C. A. Lichtenstein, F. M. Pipkin, S. W. Raither, and L. K. Sisterson. Inclusive charged-pion electroproduction. *Phys. Rev. D*, 15:3085–3104, Jun 1977.

[33] C. J. Bebek, A. Browman, C. N. Brown, K. M. Hanson, R. V. Kline, D. Larson, F. M. Pipkin, S. W. Raither, A. Silverman, and L. K. Sisterson. Longitudinal-Transverse Separation for Inclusive Electroproduction of Pions and Protons. *Phys. Rev. Lett.*, 38:1051, 1977. [Erratum: Phys.Rev.Lett. 38, 1550 (1977)].

[34] C. J. Bebek, C. N. Brown, R. V. Kline, F. M. Pipkin, S. W. Raither, L. K. Sisterson, A. Browman, K. M. Hanson, D. Larson, and A. Silverman. Electroproduction of Inclusive Pions at High Q**2. *Phys. Rev. D*, 16:1986, 1977.

[35] J. Arrington et al. Measurement of the EMC effect in light and heavy nuclei. *Phys. Rev. C*, 104(6):065203, 2021.

[36] A. Airapetian et al. Hadronization in semi-inclusive deep-inelastic scattering on nuclei. *Nucl. Phys. B*, 780:1–27, 2007.

[37] S. Moran et al. Measurement of charged-pion production in deep-inelastic scattering off nuclei with the CLAS detector. *Phys. Rev. C*, 105(1):015201, 2022.

[38] P. A. Adderley et al. The Continuous Electron Beam Accelerator Facility at 12 GeV. *Phys. Rev. Accel. Beams*, 27(8):084802, 2024.

[39] A. Karki. Ph.D Thesis, Mississippi State University, 2022.

[40] Katherine E. Myers. *The First Determination of the Proton's Weak Charge Through Parity-Violating Asymmetry Measurements in Elastic e + p and e + Al Scattering.* PhD thesis, George Washington U., 2012.

[41] Jason Seely. *Precise Measurement of the Nuclear Dependence of Structure Functions in Light Nuclei.* PhD thesis, Massachusetts Institute of Technology, Cambridge, MA (United States), 2006.

[42] Cameron William Cotton. *First Measurement of the Isospin-Dependence of Nuclear Structure Functions at 12 GeV Jefferson Lab.* PhD thesis, Univ. of Virginia, Charlottesville, VA (United States), Virginia U., 2024.

[43] Andrei Afanasev et al. Radiative corrections: from medium to high energy experiments. *Eur. Phys. J. A*, 60(4):91, 2024.

[44] M. Nycz, W. Henry, Y. Tian, W. Xiong, and X. Zheng. spokespersons, Jefferson lab experiment E12-22-004, 2022.

[45] T. Averett, A. Camsonne, X. Jiang, and N. Liyanage. spokespersons, Jefferson lab run group experiment with E12-10-006 and E12-11-108, 2014.

[46] A. Schmidt, J. C. Bernauer, V. Burkert, E. Cline, I. Korover, T. Kutz, and S. N. Santiesteban. spokespersons, Jefferson lab experiment E12+23-008 proposal, 2023.